



Published in final edited form as:

Circulation. 2008 September 16; 118(12): 1276–1284. doi:10.1161/CIRCULATIONAHA.108.789172.

Vessel-specific Toll-like receptor profiles in human medium and large arteries

Olga Pryshchep, MS¹, Wei Ma-Krupa, PhD¹, Brian R. Younge, MD², Jörg J. Goronzy, MD, PhD¹, and Cornelia M. Weyand, MD, PhD¹

¹ Lowance Center for Human Immunology and Rheumatology, Emory University School of Medicine, Atlanta, GA 30322

² Department of Ophthalmology, Mayo Clinic, Rochester, MN 55905

Abstract

Background—Inflammatory vasculopathies, ranging from the vasculitides (Takayasu arteritis, giant cell arteritis, and polyarteritis nodosa) to atherosclerosis display remarkable target tissue tropisms for selected vascular beds. Molecular mechanisms directing wall inflammation to restricted anatomical sites within the vascular tree are not understood. We have examined the ability of 6 different human macrovessels (aorta, subclavian, carotid, mesenteric, iliac, temporal arteries) to initiate innate and adaptive immune responses by comparing pathogen-sensing and T-cell stimulatory capacities.

Methods and Results—Gene expression analysis for pathogen-sensing Toll-like receptors (TLR) 1–9 showed vessel-specific profiles with TLR2 and 4 ubiquitously present, TLR7 and 9 absent, and TLR1, 3, 5, 6 and 8 expressed in selective patterns. Experiments with vessel walls stripped of the intimal or adventitial layer identified dendritic cells (DC) at the media-adventitia junction as the dominant pathogen sensors. In human artery-SCID mouse chimeras, adoptively transferred human T cells initiated vessel wall inflammation if wall-embedded DC were conditioned with TLR ligands. Wall-infiltrating T cells displayed vessel-specific activation profiles with differential production of CD40L, lymphotoxin- α , and interferon- γ . Vascular bed-specific TLR fingerprints were functionally relevant as exemplified by differential responsiveness of iliac and subclavian vessels to TLR5 but not TLR4 ligands.

Conclusions—Populated by indigenous DC, medium and large human arteries have immune sensing and T-cell stimulatory functions. Each vessel in the macrovascular tree utilizes a distinct TLR profile and supports selective T-cell responses imposing vessel-specific risk for inflammatory vasculopathies.

Keywords

arteries; immune system; inflammation

*Address for Correspondence: Cornelia M. Weyand, M.D., Ph.D., Lowance Center for Human Immunology and Rheumatology, Emory University, 101 Woodruff Circle, 1003 WMRB, Atlanta, GA 30322; telephone (404)-727-7310; fax: (404)-727-7371; e-mail: cweyand@emory.edu.

Disclosures
None.

Introduction

In contrast to microvessels, human macrovessels are complex organ systems, composed of several different wall layers, each of which is arranged from different cellular and matrix components and specifically contributes to the vessel's tasks. Structural organization of macrovessels is highly dependent on their mural thickness, which is controlled by body size and weight.¹ Therefore, it has been challenging to explore macrovascular function in experimental models as large animals are needed to mimic human body dimensions.

Macrovascular diseases display stringent target tissue tropisms and selectively affect distinctive vascular territories. Polyarteritis nodosa targets small and medium-sized arteries of the abdominal circulation.^{2, 3} Takayasu's arteritis manifests in the aorta and its primary branches, favoring neck and upper extremity vessels.⁴ Giant cell arteritis has a strong predisposition for the 2nd to 5th aortic branches and is diagnosed by biopsy of the temporal artery, a vessel of the extracranial circulation.^{5, 6} Tissue tropism for selected vascular regions is so characteristic that patterning of vascular involvement serves as an important diagnostic clue.⁷ Similarly, some arteries (coronary, carotid) are prone to develop atherosclerosis, now recognized as an inflammatory entity, whereas others (internal mammary arteries) are considered relatively resistant.

Concepts aiming to explain the predilection of selected arterial beds have assumed that vascular injury and subsequent inflammation are afflicted at the blood-wall interface, focusing attention on the macrolumen and its endothelial lining.^{8, 9} The intima is exposed to mechanical stress and circulating molecules, stressors that modulate arterial wall functionality.⁹ Also, endothelial cells (EC) have been implicated in numerous biologic and physiologic processes, ranging from antithrombotic effects to vessel tone regulation and control of inflammatory cell influx.^{9–11} However, in normal macrovessels, flow velocity may hinder adhesion and tissue migration of T cells and monocytes centrifugally into the wall. Inflammatory cells require low flow conditions, such as in capillaries, to transit into the tissue space.^{12, 13} The dominant macrovascular component is the media, a layer of concentrically arranged vascular smooth muscle cells (VSMC) and elastic membranes providing pressure resistance and elasticity. The internal elastic lamina separates the intima and media and the external elastic lamina defines the media-adventitia junction. With the exception of the human thoracic aorta, the media is avascular and thus rather inaccessible for inflammatory cells.¹⁴ However, in essentially all vasculitides, inflammatory infiltrates accumulate in the media, and the severity of media destruction largely determines patient outcome.^{4, 5}

The outermost wall layer, the adventitia, is a concentric sheet of fibroblasts, poorly organized collagenfibers, and elastic bundles. Most importantly, the adventitia holds a microvascular network, or vasa vasorum, which supplies oxygen and nutrients to the wall. The adventitia functions critically in immune recognition and regulating vascular inflammation.^{15–17} Specifically, dendritic cells (DC) in the adventitia recognize pathogen-derived molecular patterns and initiate adaptive immune responses in an otherwise immunoprivileged niche.¹⁸ Collar-induced occlusion of vasa vasorum causes rapid intimal hyperplasia, emphasizing the adventitia's regulatory role in global vascular function.¹⁹

The current study explored whether human macrovessels as organs settled by endogenous DC participate in innate and adaptive immunity. More importantly, we examined whether arteries from distinct vascular territories display heterogeneity in their immune-regulatory functions, providing a possible clue toward the tissue tropisms of inflammatory vasculopathies. Innate and adaptive immune processes are involved in the atherosclerotic plaque and in large-vessel vasculitis. In the plaque, both myeloid and plasmacytoid DC respond to microbial patterns and modulate tissue destructive immune responses,^{20, 21} including TRAIL-mediated T-cell

cytotoxicity.²² In GCA, CD83⁺ DC depletion abrogates vasculitis, attesting to the critical role of activated DC in sustaining wall inflammation.¹⁸ Less is known about DC populations in normal, non-inflamed arteries. Initial attention focused on a subintimal DC network in human aorta and carotid arteries first described by Bobryshev as S-100⁺ cells with a characteristic DC-like ultrastructure.²³ Wick and colleagues have described vascular DC in the intima of normal, non-atherosclerotic arteries and have introduced the vascular-associated lymphoid tissue (VALT) concept.^{24, 25} The current project has focused on the larger family of human macrovessels, including subclavian, mesenteric, iliac, and temporal arteries. These macrovessels are occupied by DC embedded deep in the wall, specifically in the adventitia where they co-localize with the vasa vasorum network and lymphatic vessels. Endowed with pattern-recognition receptors of the Toll-like receptor (TLR) family, adventitial vascular DC empower the vessel wall with pathogen-sensing functions, which widen the role of macroarterial tissues far beyond the transport of blood and blood pressure regulation.

Methods

Tissue specimens

Human arteries with intact wall structures were collected during postmortem examinations of 37 donors (mean age 64 years; 25 males, 12 females). Samples were harvested within 8 hours of death from 6 vascular beds (temporal, carotid, subclavian, mesenteric, iliac, and thoracic aorta). Fresh blood vessels were obtained from diagnostic biopsies or vascular repair procedures and were immediately shock frozen or embedded in OCT. Based on histomorphologic examination, only samples with normal wall structure without atherosclerotic lesions and inflammatory infiltrates were selected. To ensure consistent and high quality of vascular tissues, minimal β -actin transcript expression per mm³ of was set at 6×10^5 copies. Selective degradation of gene transcripts in the autopsy specimens was ruled out by direct comparison of TLR profiles in postmortem samples and tissues obtained during surgical procedures (Supplemental Figure 1). Kinetic experiments in which aortic wall was stored for 30 hours after acquisition confirmed stability of TLR expression profiles postmortem (Supplemental Figure 2) as previously reported.²⁶ All protocols were approved by the Emory University Institutional Review Board.

q-PCR

Total RNA was isolated from shock frozen tissues using TRIzol (Invitrogen, Carlsbad, CA), reverse transcribed into cDNA using AMV reverse transcriptase (Roche Applied Sciences, Indianapolis, IN), and amplified with specific primer pairs (Supplemental Table 1) as described previously.²²

Immunohistochemistry

Slides were prepared as previously described.¹⁸ Antibodies are listed in Supplemental Table 2. After blocking with 5% normal goat serum, tissue sections were incubated with primary antibodies (CD11c, TLR2, TLR4, TLR5, CD86) for 1 hour followed by biotin-conjugated secondary antibody for 30 min, and ABC-Elite solution (Vector Laboratories, Burlingame, CA). Binding was visualized using the chromagen 3,3'-diaminobenzidine (Dako, Carpinteria, CA). For dual-color staining, slides were again blocked with serum, and incubated with primary antibody (von Willebrand Factor, vWF) and then secondary (sheep-anti-rabbit) antibody for 60 and 30 min, respectively. Sections were developed with ABC-alkaline phosphatase and visualized using red chromagens (Vector Laboratories). Endogenous alkaline phosphatase activity was inhibited with levamisole. Slides were counterstained with hematoxylin (Surgipath, Richmond, IL). Control stains with isotype-matched primary Abs were included in each experiment.

Blood vessel organ culture

Arteries were cut into rings and placed into 48-well plates filled with complete medium (RPMI, 10% fetal calf serum). For “partial wall” experiments, either the endothelial or adventitial layer was stripped off. Tissues were stimulated with LPS (1µg/mL, Sigma-Aldrich, St. Louis, MO) or flagellin (1µg/mL, InvivoGen, CA), or left untreated for 24 hours. Subsequently, arteries were shock frozen for RNA isolation or OCT embedded for immunohistochemistry.

In vivo stimulation of human arteries

Arteries were subcutaneously implanted on the lower midback of NOD.CB17 Prkdc (SCID) mice.¹⁸ 7 days after implantation, chimeras were injected with LPS (3µg/mouse IP) or PBS. 24 hours later, CD4⁺ T cells from healthy donors were adoptively transferred into each mouse (20×10⁶/mouse, IV). One week later, the artery grafts were recovered and shock frozen for RNA isolation. For DC depletion, arterial tissues were treated with GdCl₃ (300µg/ml, Sigma-Aldrich) for 1 hour prior to implantation. All procedures were approved by the Animal Care and Use Committee.

In vivo T-cell tracking

CD4⁺ T cells were isolated from healthy donors and labeled with 2 µM PKH67 green fluorescence dye (Sigma, St. Louis, MO). Labeled cells were adoptively transferred into human artery-SCID chimeras as described.²⁷ 7 µm acetone-fixed tissue sections from explanted arteries were mounted in DAPI containing Vectashield (Vector Laboratories, Inc.). Images from two fluorescence channels were merged using Adobe Photoshop 7.0.1. PKH67⁺ tissue-infiltrating cells were counted in 5 high powered fields (HPF) per section in 5 non-serial sections.

Data analysis

Data were analyzed by one-way and two-way ANOVA using Sigma Stat 3.1 software. In the transcriptome profiling studies, relative TLR expression was obtained by normalization of each TLR to the median of all samples. Heat plots were generated using GeneSpring software.

Statement of Responsibility

The authors had full access to and take full responsibility for the integrity of the data. All authors have read and agree to the manuscript as written.

Results

1. Blood vessel-specific expression profiles for Toll-like receptors

The precise patterning in which inflammatory vasculitides target macrovessels suggests an active contribution of the vessel wall itself. Inflammation begins with the activation of innate immune responses, followed by formation of adaptive immunity. Pattern recognition receptors, e.g. TLR, initiate immune responses by sensing microbial motifs. We therefore established receptor expression profiles for TLR1-9 in tissue samples from 6 arterial territories (Fig. 1). Transcripts for each TLR were quantified in each tissue by qPCR. Remarkably, TLR profiles were heterogeneous and strongly correlated with the artery’s anatomical origin (Fig. 1).

TLR expression levels were significantly different ($p < 0.001$) when the 6 vascular territories were compared. TLR2 had the highest copy numbers with significantly different expression among the 6 different arteries ($p < 0.001$). TLR4 was also abundantly expressed; levels in the 6 vascular beds were not statistically different. TLR7 and TLR9 were produced at low levels with only iliac arteries containing intermediate amounts (n.s.). TLR1 demonstrated remarkable selectivity dividing the arteries into high (iliac, aorta, carotid) and low (temporal, subclavian,

mesenteric) expressers ($p < 0.05$ iliac vs. any low-expressing artery). TLR1 and TLR6 had similar distribution patterns with high expression in aortic, carotid, and iliac samples and 5 to 10-fold lower transcript levels in mesenteric, subclavian, and temporal arteries. TLR5-specific sequences varied significantly amongst the arterial territories ($p < 0.001$). TLR3 displayed a selective expression pattern: carotid and aorta were positive; temporal and iliac vessels were essentially negative ($p < 0.005$). Similarly, TLR8 expression varied widely with temporal and iliac arteries positive but mesenteric and aorta negative ($p < 0.05$). Carotid samples were an exception; they contained similar levels of TLR3 and TLR8 transcripts ($p = 0.2$).

In a different approach to comparing expression of TLR family members, we used an artery-centric view (Fig. 1B). The TLR profile of iliac arteries was distinct from that of all other vessels ($p < 0.001$) and had the broadest TLR spectrum with 8 of 9 family members present (all except TLR3). Carotid arteries contained 7 of the 9 TLR types, missing TLR7 and TLR9. The aorta's signature pattern was high levels of TLR1-6. The carotid and aortic patterns were statistically not different (Fig. 1). The TLR portfolio was less diverse in mesenteric and subclavian arteries which appeared alike. Temporal arteries had an unusual pattern with high amounts for TLR2, 4, and 8 and intermediate results for TLR1, 5, and 6. The biggest difference in TLR profile, both in pattern and expression levels, was observed between iliac and subclavian vessels ($p < 0.001$). TLR profiles did not correlate with donor age, sex, or body mass index (data not shown).

2. TLR⁺ DC distribution in the major human arteries

TLR are typically expressed on DC but can appear on other cell types, especially monocytes, macrophages, and B cells. Also, non-immune cells in the arterial wall, such as EC and VSMC could contribute to TLR expression. To explore which immune cells are represented in human macrovessels, we screened for cell-type specific markers by qPCR (Fig. 2). All arteries expressed abundant transcripts for the DC marker CD11c. Arterial extracts were essentially negative for T-cell receptor transcripts, macrophage-specific CD11b transcripts, and the B-cell marker CD79A with transcript levels below 10 copies per 200,000 β -actin transcripts. The exceptions were iliac vessels in which low levels (10–100 copies) of these markers were detectable. These experiments essentially limited the spectrum of professional wall-residing immune cells to DC. The 6 vascular beds displayed a clear hierarchy of CD11c expression (Fig. 2). The aorta, the carotids, and the iliac arteries shared high levels of CD11c transcripts. Mesenteric, subclavian, and temporal vessels had lower levels of CD11c-specific sequences ($p < 0.05$, compared to aorta). CD11c representation was unrelated to vessel diameter or elasticity; specifically, subclavian arteries resembled temporal arteries although subclavians have wall characteristics comparable to carotids.

The precise placement of CD11c⁺ cells in the wall layers was determined by double staining tissue sections for the endothelial marker van Willebrand factor (vWF) and the DC marker CD11c (Fig. 2). All vessels had a circumferential ring of CD11c⁺ cells positioned at the adventitia-media border. CD11c⁺ cells within the medial VSMC layer were isolated and rare. Only the aorta and the carotid had an additional set of CD11c⁺ DC within the intimal stratum. In temporal, mesenteric, iliac and subclavian arteries, such intimal DC were rarely encountered. Thus, adventitial CD11c⁺ DC are a common feature of all human macrovessels (Supplemental Table 3). Only aortic and carotid walls possess additionally an intimal DC network.

3. Macroarteries sense TLR ligands in vitro and in vivo and respond with DC activation and in situ T-cell stimulation

To test the functional relevance of wall-embedded TLR-expressing cells, we concentrated on TLR2 and 4, receptors consistently encountered in all vessels. Immunohistochemistry for TLR2 and TLR4 localized positive cells at the media-adventitia border (Fig. 3). Dual-color

staining with the endothelial marker vWF distinguished TLR4⁺ cells from vasa vasorum EC. EC lining the macrolumen gave a low and inconsistent signal for binding of TLR4-reactive antibodies and were uniformly negative for TLR2. Also, in all arterial sections, medial VSMC lacked TLR2 and TLR4 expression. These results focused interest on adventitial DC as TLR sensors.

To test vascular TLR functional relevance, arteries were exposed to TLR4 ligands either in organ culture or after engrafting the human vessels into SCID chimeras. PKH67-labeled CD4⁺ T cells were adoptively transferred into human artery-SCID mouse chimeras. In-vitro stimulation of arterial wall patches with LPS for 24 hours promptly resulted in transcriptional upregulation of the DC activation markers CD83 and CD86 (Fig. 4A). Immunohistochemistry identified CD86⁺ cells exclusively in the adventitia (Fig. 4B). Similarly, human arteries recovered from mouse chimeras upregulated CD83, CD86, and CCL19, the T-cell attracting chemokine produced by activated DC (Fig. 4C). Explanted arteries contained high levels of TCR-specific transcripts, and immunohistochemistry visualized intramural CD4 T cells (Fig. 4D), confirming that TLR triggering paved the way for adaptive immune responses. Recruited T cells underwent in situ stimulation as evidenced by the induction of early and intermediate T-cell activation markers including CD40L, lymphotoxin-alpha (LT α), and interferon-gamma (IFN γ) (Fig. 4C). Subclavian arteries were the most potent in eliciting LT α production. In contrast, carotid arteries outperformed subclavian and iliac arteries in inducing IFN γ production. All three arterial beds equally upregulated the early T-cell activation marker CD40L.

Venous tissues were essentially non-responsive to TLR ligands. In contrast to arteries, stimulation of mesenteric veins in organ culture with LPS failed to induce both CD83 and CD86 (Supplemental Table 4).

4. Adventitial DC are key regulators of LPS responsiveness

To test pathogen-sensing functions of different wall layers, we studied TLR4 responsiveness in partially denudated vessels. The adventitial or intimal layers were carefully removed; denudation accuracy was confirmed with anti-vWF staining (Fig. 5A). Denudated or intact arteries were stimulated with LPS in organ culture, and activation was assessed by quantifying CD86 induction. Denudation of macroluminal EC did not diminish LPS-induced CD86 upregulation. Conversely, stripping of the adventitial layer essentially abrogated LPS sensing. Immunohistochemical studies in LPS-treated arteries confirmed that CD86 was exclusively expressed on adventitial CD11c⁺ cells (Fig. 5B), identifying adventitial cells as critical mediators of TLR recognition. To provide further evidence for adventitial DC as the artery's sentinels, we proceeded with depletion experiments targeting phagocytic cells. Amongst the different cell types composing the normal vessel wall (VSMC, EC, fibroblasts, vascular DC), only DC are capable of phagocytosis. At branching points, some arteries may contain macrophages with phagocytic capability. Vessel segments examined in this study lacked wall-residing macrophages as documented by the absence of CD11b transcripts (Fig. 2). To deplete phagocytes, human arteries were pretreated with gadolinium (III) chloride just prior to implantation. Chimeras were injected with LPS followed by adoptive transfer of human CD4 T cells (Fig. 5C). Phagocyte-depleted arteries were markedly impaired in responding to LPS ($p < 0.001$ LPS vs. Gd/LPS). DC activation markers CD83, CD86, and CCL19 showed minimal induction, assigning all three markers to phagocytic cells. In the absence of phagocytic cell activation, T-cell attraction (Fig. 5C) and in situ T-cell activation (CD40L) was abrogated.

5. Heterogeneous TLR expression profiles predict differential response patterns to pathogen-derived motifs

The TLR transcriptome comparative analysis (Fig. 1) suggested vessel-specificity and macrovascular bed heterogeneity. Essentially all arteries shared TLR4 expression (Fig. 1 and 3) and were capable of sensing TLR4 ligands. Other TLR, such as TLR3 and TLR5, displayed marked variability with high- and low-expressing vascular territories. To examine whether differences in expression profiles translated into functional consequences, we compared responsiveness to TLR4 and TLR5 ligands in subclavian and iliac arteries which lack a sub-endothelial DC network. Based on transcript levels, both artery types were predicted to react to LPS but display differential responsiveness to the TLR5 ligand flagellin.

Immunohistochemistry identified TLR5-positive cells exclusively in the adventitia in both arteries, with much higher frequencies in iliac vessels (Fig. 6). Multifold induction of CD83 and CD86 transcripts demonstrated robust subclavian and iliac DC activation in response to LPS (Fig. 6) ($p < 0.05$ for both markers in both vessels compared to control). In contrast, flagellin was a powerful activator for iliac vessels ($p < 0.001$) but was ineffective in stimulating subclavian DC. Thus, TLR expression patterns not only provided a unique fingerprint for each arterial territory, but also predicted the vessel's ability to sense and react to pathogen-derived motifs.

Discussion

Besides their role in transporting blood, arteries have numerous physiologic functions, including regulation of blood pressure and blood coagulability. Many of these functions have been assigned to EC lining the lumen. Much less is known about distal wall layers. Data presented here establish human macrovessels as lymphoid organs, equipped with sophisticated DC networks that have sensing function and monitor host exposure to pathogens through pattern recognition receptors. Remarkably, macrovessels from different vascular territories express vessel-specific profiles of pathogen-sensing TLR suggesting functional specialization in the surveillance task of arteries, with each region of the vascular tree dedicated to a selected spectrum of TLR ligands. This specialization of blood vessel territories mirrors the stringent target tissue tropism of inflammatory vasculopathies. Clinicians have long been puzzled by the selective distribution pattern of vasculopathies, including vasculitides and atherosclerosis.²⁸ Here, we propose that vessel wall determinants may direct disease processes to unique sites. Conceptualizing macrovessels as a lymphoid tissue markedly extends the scope of the immune system's monitoring capabilities and implicates macrovessels as immunomodulators that regulate not only local but also systemic immune responses.

Data presented here strongly support that large arteries sense circulating molecules through more than their EC layers. Determined by body size, structuring of deeper wall layers is different in small animals and humans. The number of aortic smooth muscle cell lamellae is tightly correlated to overall body size. Media thickness dictates the need for the adventitial vasa vasorum network¹, the major access route for cells to the vessel wall. Notably, lymphocytes egress from the blood into tissue through high endothelial venules, after the blood has passed the capillaries.²⁹ Vessel wall-residing DC in the aorta and carotid artery have been suspected to contribute to vascular pathology. Wick and colleagues have demonstrated their presence in healthy young individuals, long before atherosclerotic streaks appear,²⁴ giving rise to the model of a vascular-associated lymphoid tissue (VALT), comparable to mucosa-associated lymphoid tissue (MALT).³⁰ Subendothelial DC may advance atherosclerosis,³⁰ but it is unknown how they function. In our experiments, CD4 T cells did not selectively accumulate in the subintima. Whether T cells can reach subintimal DC as long as the vessel wall is intact and avascular is unknown but would involve migration throughout the entire wall. This scenario obviously changes dramatically once a plaque is established, capillary support

is remodeled, and the media and intima are easily accessible for T cells.^{31, 32} In the plaque, highly activated DC co-localize with T cells and produce T cell-attracting chemokines.³³

Partial wall experiments assigned pathogen sensing in normal vessels primarily to adventitial DC. TLR expression patterns identified wall-residing DC as myeloid-like, recognizing bacterial products. Whether wall-residing DC fall into several subcategories requires more detailed molecular profiling. So far, we have failed to find plasmacytoid DC (pDC) in normal vessels; they are abundant in the atherosclerotic plaque where they release IFN- α upon triggering with TLR9 ligands.³⁴

In the gene expression studies comparing whole wall-derived transcript pools, cells others than DC could obviously contribute to the TLR pattern. TLR4 expression has been described for EC and VSMC when associated with the atherosclerotic plaque. However, in normal, non-inflamed arteries VSMC are consistently negative for TLR4 staining.³⁵ Macroluminal EC show weak and inconsistent binding of TLR4-staining, with no CD86 induction upon LPS stimulation. The partial wall experiments and the in vivo experiments strongly implicated adventitial DC as the major sensors of pathogen-related motifs.

The questions arise as to why macrovessels participate in pathogen sensing and why vascular territories specialize in selected TLR portfolios. Studies with temporal arteries^{18, 36} and other macroarteries described here unequivocally demonstrate that in their physiologic state wall-embedded DC do not initiate immune responses. TLR stimulation is necessary to render wall-residing DC immunogenic.¹⁸ Thus, vascular DC are primarily tolerogenic, protecting the artery from inflammatory attack. Considering the vital role of macrovessels and the small margin of benefit gained by vessel inflammation, this immunologic niche is definitely preferable. This niche appears not only to be defined by structural determinants, such as accessibility, but actively maintained by wall-resident DC.

Vascular territory specialization in sensing pathogens may be related to anatomical positioning. Iliac arteries are near the gut; monitoring for flagellin may provide advantage. This concept assumes far-reaching contact and communication between arteries and their tissue environment. Interestingly, veins which carry blood away from organs lack DC (see also Supp. Table 4). Alternatively, DC placed around vasa vasorum may contribute to absorbing circulating endotoxins. Patients undergoing teeth cleaning display prolonged endothelial dysfunction following vascular tree exposure to subclinical bacteremia.³⁷ Traditionally, EC have been implicated in sensing such danger signals; current data suggest that wall-embedded DC play a major role in this vascular sensing function.

Experimental approaches of this study (in vitro organ culture and xenograft model) were focused on pathogen-sensing functions of the wall, with TLR ligands reaching wall-embedded cells through vasa vasorum. Flow conditions in the macrolumen were not investigated. As TLR sensing was not affected by intima stripping but was essentially eliminated by adventitia removal (Fig. 5), cells seated deep in the wall structure must be primarily responsible for TLR ligand recognition.

In vivo experiments demonstrating that human macrovessels are capable of supporting T-cell recruitment and in situ activation suggest broader immunoregulatory function of arteries. This places vascular DC into a critical position. As guardians of the artery's wall, they can protect the structural integrity of these vital and non-regenerative tissue structures. If appropriately triggered though, vascular DC can initiate and sustain vessel wall inflammation, assigning them a checkpoint role in vasculitis. Diversity in TLR profile of human macrovessels provides a molecular framework for the selective targeting of vascular beds with the potential to identify unique instigators and therapeutic modalities for different vasculitides. Finally, vascular DC

may provide immunoregulatory functions affecting not only local but also systemic immune responses.

Supplementary Material

Refer to Web version on PubMed Central for supplementary material.

Acknowledgments

The authors thank the National Disease Research Interchange, the Georgia Eye Bank, and their colleagues in the Departments of Surgery and Pathology at Emory University for providing human artery samples. The authors thank Tamela Yeargin for manuscript editing.

Funding Sources

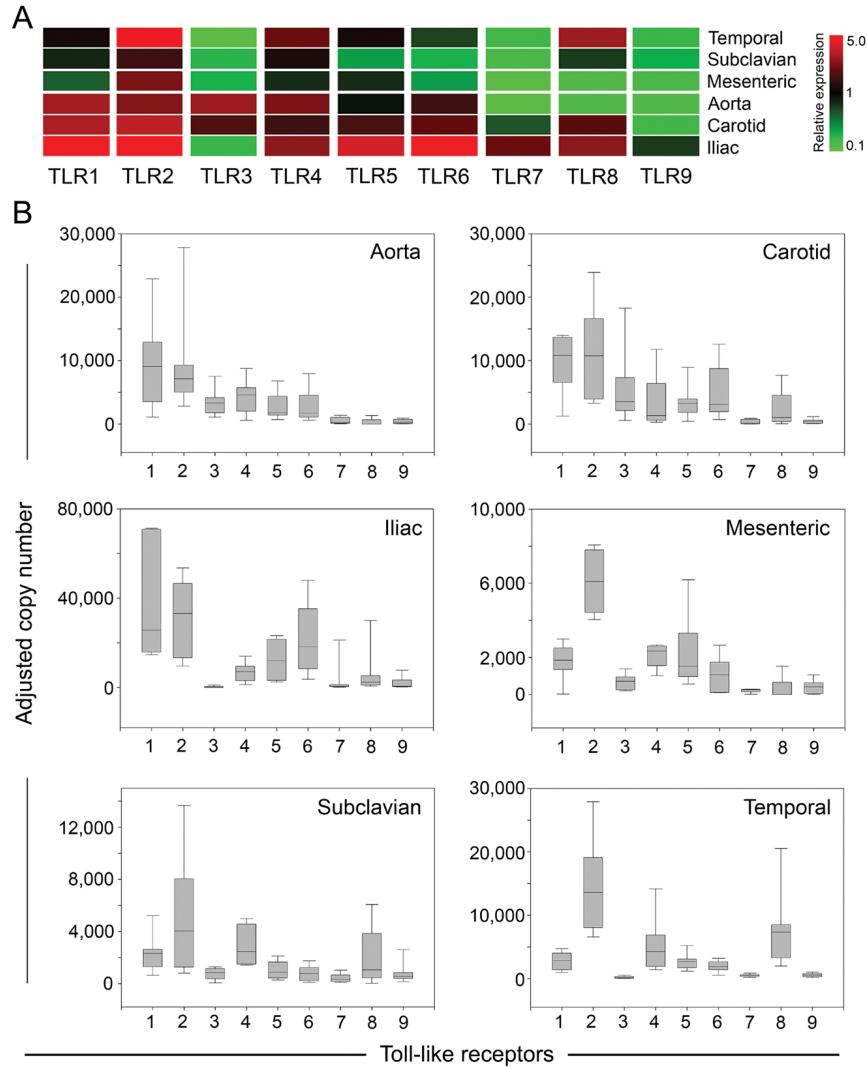
This work was funded in part by the National Institutes of Health (RO1 EY11916, RO1 AR42527 and RO1 AI44142), the Dana Foundation, and the McIntyre Family Discovery Fund.

References

1. Wolinsky H, Glagov S. Nature of species differences in the medial distribution of aortic vasa vasorum in mammals. *Circ Res* 1967;20:409–421. [PubMed: 4960913]
2. Zeek PM. Periarteritis nodosa; a critical review. *Am J Clin Pathol* 1952;22:777–790. [PubMed: 14943695]
3. Morgan MD, Savage CO. Vasculitis in the gastrointestinal tract. *Best Pract Res Clin Gastroenterol* 2005;19:215–233. [PubMed: 15833689]
4. Burke AP, Tavora F, Narula N, Tomaszewski JE, Virmani R. Aortitis and ascending aortic aneurysm: description of 52 cases and proposal of a histologic classification. *Hum Pathol* 2008;39:514–526. [PubMed: 18294676]
5. Weyand CM, Goronzy JJ. Medium- and large-vessel vasculitis. *N Engl J Med* 2003;349:160–169. [PubMed: 12853590]
6. Hoffman GS. Large-vessel vasculitis: unresolved issues. *Arthritis Rheum* 2003;48:2406–2414. [PubMed: 13130459]
7. Mandell BF, Hoffman GS. Differentiating the vasculitides. *Rheum Dis Clin North Am* 1994;20:409–442. [PubMed: 8016419]
8. Tesfamariam B, DeFelice AF. Endothelial injury in the initiation and progression of vascular disorders. *Vascul Pharmacol* 2007;46:229–237. [PubMed: 17218160]
9. Trepels T, Zeiher AM, Fichtlscherer S. The endothelium and inflammation. *Endothelium* 2006;13:423–429. [PubMed: 17169774]
10. Bacon PA. Endothelial cell dysfunction in systemic vasculitis: new developments and therapeutic prospects. *Curr Opin Rheumatol* 2005;17:49–55. [PubMed: 15604904]
11. Cines DB, Pollak ES, Buck CA, Loscalzo J, Zimmerman GA, McEver RP, Poer JS, Wick TM, Konkle BA, Schwartz BS, Barnathan ES, McCrae KR, Hug BA, Schmidt AM, Stern DM. Endothelial cells in physiology and in the pathophysiology of vascular disorders. *Blood* 1998;91:3527–3561. [PubMed: 9572988]
12. Miyasaka M, Tanaka T. Lymphocyte trafficking across high endothelial venules: dogmas and enigmas. *Nat Rev Immunol* 2004;4:360–370. [PubMed: 15122201]
13. Steeber DA, Tedder TF. Adhesion molecule cascades direct lymphocyte recirculation and leukocyte migration during inflammation. *Immunol Res* 2000;22:299–317. [PubMed: 11339364]
14. Dal Canto AJ, Swanson PE, O'Guin AK, Speck SH, Virgin HW. IFN-gamma action in the media of the great elastic arteries, a novel immunoprivileged site. *J Clin Invest* 2001;107:R15–22. [PubMed: 11160143]
15. Hildebrandt HA, Goessl M, Mannheim D, Versari D, Herrmann J, Spendlove D, Bajajowski T, Malyar NM, Erbel R, Lerman LO, Lerman A. Differential distribution of vasa vasorum in different vascular beds in humans. *Atherosclerosis*. 2007

16. Wagner AD, Bjornsson J, Bartley GB, Goronzy JJ, Weyand CM. Interferon-gamma-producing T cells in giant cell vasculitis represent a minority of tissue-infiltrating cells and are located distant from the site of pathology. *Am J Pathol* 1996;148:1925–1933. [PubMed: 8669478]
17. Weyand CM, Ma-Krupa W, Pryshchep O, Groschel S, Bernardino R, Goronzy JJ. Vascular dendritic cells in giant cell arteritis. *Ann N Y Acad Sci* 2005;1062:195–208. [PubMed: 16461802]
18. Ma-Krupa W, Jeon MS, Spoerl S, Tedder TF, Goronzy JJ, Weyand CM. Activation of arterial wall dendritic cells and breakdown of self-tolerance in giant cell arteritis. *J Exp Med* 2004;199:173–183. [PubMed: 14734523]
19. De Meyer GR, Van Put DJ, Kockx MM, Van Schil P, Bosmans R, Bult H, Buysens N, Vanmaele R, Herman AG. Possible mechanisms of collar-induced intimal thickening. *Arterioscler Thromb Vasc Biol* 1997;17:1924–1930. [PubMed: 9351355]
20. Niessner A, Shin MS, Pryshchep O, Goronzy JJ, Chaikof EL, Weyand CM. Synergistic Proinflammatory Effects of the Antiviral Cytokine Interferon- α and Toll-Like Receptor 4 Ligands in the Atherosclerotic Plaque. *Circulation* 2007;116:2043–2052. [PubMed: 17938289]
21. Doherty TM, Fisher EA, Arditi M. TLR signaling and trapped vascular dendritic cells in the development of atherosclerosis. *Trends Immunol* 2006;27:222–227. [PubMed: 16580258]
22. Sato K, Niessner A, Kopecky SL, Frye RL, Goronzy JJ, Weyand CM. TRAIL-expressing T cells induce apoptosis of vascular smooth muscle cells in the atherosclerotic plaque. *J Exp Med* 2006;203:239–250. [PubMed: 16418392]
23. Bobryshev YV, Lord RS. S-100 positive cells in human arterial intima and in atherosclerotic lesions. *Cardiovasc Res* 1995;29:689–696. [PubMed: 7606759]
24. Millonig G, Niederegger H, Rabl W, Hochleitner BW, Hofer D, Romani N, Wick G. Network of vascular-associated dendritic cells in intima of healthy young individuals. *Arterioscler Thromb Vasc Biol* 2001;21:503–508. [PubMed: 11304464]
25. Millonig G, Schwentner C, Mueller P, Mayerl C, Wick G. The vascular-associated lymphoid tissue: a new site of local immunity. *Curr Opin Lipidol* 2001;12:547–553. [PubMed: 11561175]
26. Sanoudou D, Kang PB, Haslett JN, Han M, Kunkel LM, Beggs AH. Transcriptional profile of postmortem skeletal muscle. *Physiol Genomics* 2004;16:222–228. [PubMed: 14625377]
27. Zhang X, Nakajima T, Goronzy JJ, Weyand CM. Tissue trafficking patterns of effector memory CD4⁺ T cells in rheumatoid arthritis. *Arthritis Rheum* 2005;52:3839–3849. [PubMed: 16329093]
28. Hoffman GS. Determinants of vessel targeting in vasculitis. *Ann N Y Acad Sci* 2005;1051:332–339. [PubMed: 16126975]
29. Picker LJ, Butcher EC. Physiological and molecular mechanisms of lymphocyte homing. *Annu Rev Immunol* 1992;10:561–591. [PubMed: 1590996]
30. Wick G, Romen M, Amberger A, Metzler B, Mayr M, Falkensammer G, Xu Q. Atherosclerosis, autoimmunity, and vascular-associated lymphoid tissue. *Faseb J* 1997;11:1199–1207. [PubMed: 9367355]
31. Moreno PR, Purushothaman KR, Zias E, Sanz J, Fuster V. Neovascularization in human atherosclerosis. *Curr Mol Med* 2006;6:457–477. [PubMed: 16918368]
32. Moulton KS. Angiogenesis in atherosclerosis: gathering evidence beyond speculation. *Curr Opin Lipidol* 2006;17:548–555. [PubMed: 16960504]
33. Erbel C, Sato K, Meyer FB, Kopecky SL, Frye RL, Goronzy JJ, Weyand CM. Functional profile of activated dendritic cells in unstable atherosclerotic plaque. *Basic Res Cardiol* 2007;102:123–132. [PubMed: 17136419]
34. Niessner A, Sato K, Chaikof EL, Colmegna I, Goronzy JJ, Weyand CM. Pathogen-sensing plasmacytoid dendritic cells stimulate cytotoxic T-cell function in the atherosclerotic plaque through interferon- α . *Circulation* 2006;114:2482–2489. [PubMed: 17116765]
35. Edfeldt K, Swedenborg J, Hansson GK, Yan ZQ. Expression of toll-like receptors in human atherosclerotic lesions: a possible pathway for plaque activation. *Circulation* 2002;105:1158–1161. [PubMed: 11889007]
36. Ma-Krupa W, Kwan M, Goronzy JJ, Weyand CM. Toll-like receptors in giant cell arteritis. *Clin Immunol* 2005;115:38–46. [PubMed: 15870019]

37. Tonetti MS, D'Aiuto F, Nibali L, Donald A, Storry C, Parkar M, Suvan J, Hingorani AD, Vallance P, Deanfield J. Treatment of periodontitis and endothelial function. *N Engl J Med* 2007;356:911–920. [PubMed: 17329698]



p-values for pairwise comparisons of TLR distributions

	Carotid	Subclavian	Mesenteric	Iliac	Temporal
Aorta	0.982	0.026	0.205	0.002	0.001
Carotid		0.008	<0.001	<0.001	0.001
Subcl			0.660	<0.001	<0.001
Mesent				<0.001	0.003
Iliac					<0.001

Figure 1. Expression patterns of TLR family members in distinct vascular territories

Total RNA was extracted from human aortas (n=15 different donors), carotid (n=15), iliac (n=11), mesenteric (n=15), subclavian (n=15), and temporal arteries (n=13), and transcript numbers for each TLR were measured by quantitative RT-PCR (A). Relative expression was obtained by normalizing TLR levels for each vascular bed to the median of all samples. Red fields represent higher than average expression levels; green fields denote below average transcript expression. (B) Transcript numbers for each individual TLR in each vascular bed normalized to β -actin copies are presented as box plots with medians, 25th and 75th percentiles as boxes, and 10th and 90th percentiles as whiskers. p values for pairwise comparisons of TLR expression patterns amongst the 6 arterial territories are shown.

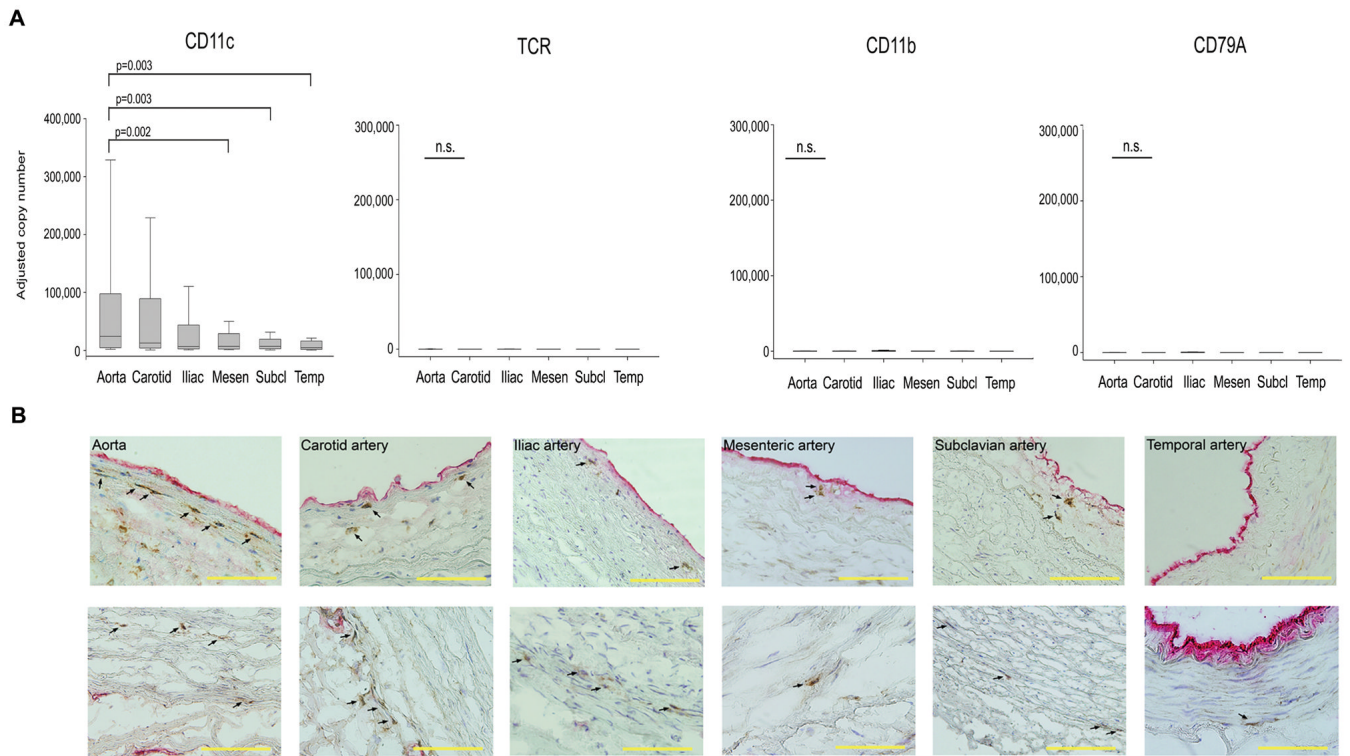


Figure 2. Immune cell populations in major human arteries

(A) Samples from human arteries were collected as described in Fig. 1, and mRNA levels for the cell-type specific markers CD11c, T-cell receptor (TCR), CD11b, and the B-cell marker CD79A were quantified by RT-PCR. Results are shown as box plots with medians, 25th and 75th percentiles as boxes, and 10th and 90th percentiles as whiskers. (B) Physical localization of CD11c⁺ vascular dendritic cells within the arterial wall was assessed by immunohistochemistry. Frozen sections of the different vascular specimens were doublestained with antibodies specific for CD11c (brown) and the endothelial cell marker vWF (red). Vascular DC localized within the intima (top), and at the media-adventitia border (bottom) are highlighted by arrows. Scale bar: 100µm.

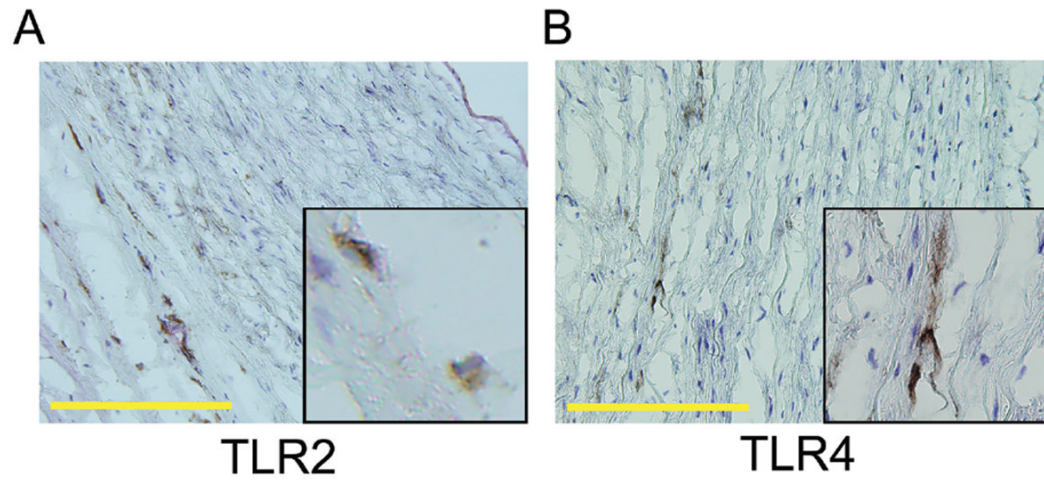


Figure 3. TLR2 and TLR4 protein expression within the normal vascular wall

Arterial cross-sections were stained with antibodies specific for TLR2 or TLR4. Representative stains for subclavian (**A**) and iliac artery (**B**) are shown. (DAB, brown, magnification $\times 200$, inset magnifications $\times 400$). TLR2- or TLR4-expressing cells were predominantly found along the media-adventitia border. Scale bar: 100 μ m.

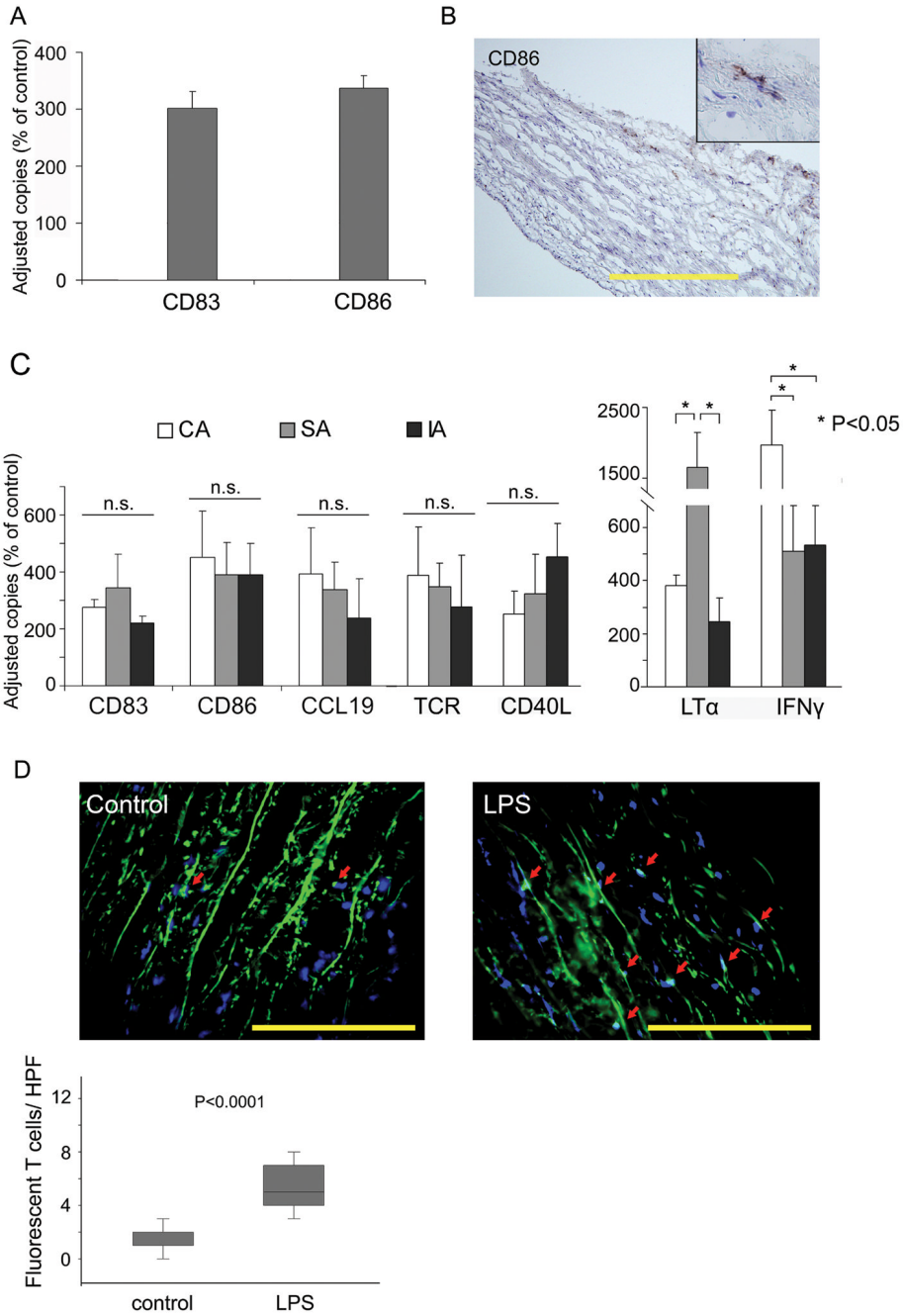


Figure 4. Vascular DC sense TLR4 ligands in vitro and in vivo

(A) Subclavian arteries were with or without LPS (1 μ g/ml) for 12 hours in vitro. mRNA from tissue extracts were analyzed for CD83 and CD86 expression by RT-PCR. Copy numbers of the target mRNA are presented as percent of untreated control. Results from 1 of 5 experiments are shown as mean \pm SD of triplicate measurements. (B) LPS-induced expression of CD86 protein was restricted to DC at the media-adventitia border. Frozen sections were stained with anti-CD86 and developed with DAB (magnification \times 200, inset magnification \times 400). Scale bar: 100 μ m. (C) Carotid (open bars), subclavian (gray bars), and iliac (black bars) arteries were engrafted into SCID mice. Chimeras received LPS (3 μ g/mouse) or PBS by i.p. injection. Human CD4⁺ T cells were adoptively transferred 24 hours later into all mice. Grafts were

explanted and markers of DC activation (CD83, CD86, CCL19) and T-cell recruitment (TCR) and in-situ activation (CD40L, LT α , IFN γ) were quantified by RT-PCR. Results are presented as percent of sham-treated control. **(D)** CD4 T cells were labeled with PKH67 prior to adoptive transfer. Human subclavian artery grafts were explanted, and fluorescent T cells infiltrating into the grafts were quantified in 25 randomly chosen HPF. Results are shown as box plots with medians, 25th and 75th percentiles as boxes, and 10th and 90th percentiles as whiskers. Scale bar: 50 μ m.

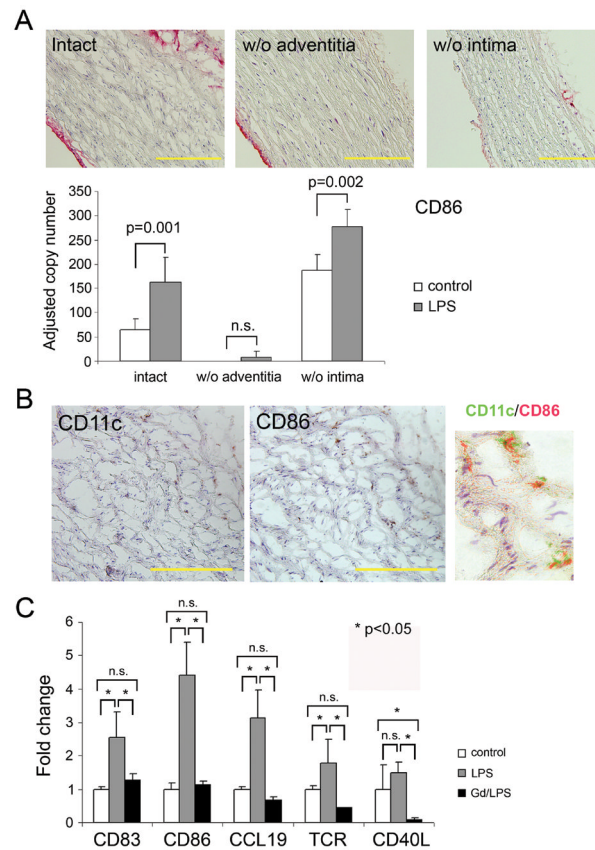


Figure 5. Pathogen sensing is a function of the adventitia, not the intima

(A) Partial walls from subclavian arteries were generated by stripping off either the intima or the adventitia. Efficiency of denudation was monitored by staining for endothelial vWF (red stain). Scale bar: 100 μ m. Intact and partial vessel walls were stimulated with LPS for 24 hours. CD86 mRNA was quantified by RT-PCR, and results from 5 experiments are shown as mean \pm SD. (B) Induction of CD86 protein on CD11c⁺ adventitial DC was assessed by immunohistochemistry on serial slides. To confirm co-localization, pseudocolored sections were merged. Scale bar: 50 μ m. (C) Dendritic cells were depleted from intact vessel walls by incubation with gadolinium (III) chloride (Gd). Vessels were subsequently engrafted into SCID mice. DC and T-cell functions were evaluated after LPS injection and adoptive transfer of human CD4 T cells. DC activation markers (CD83, CD86, CCL19) and T-cell markers (TCR, CD40L) were quantified in explanted human arteries by RT-PCR and are presented as fold change compared to untreated controls. Results from 1 of 3 independent experiments are shown as mean \pm SD.

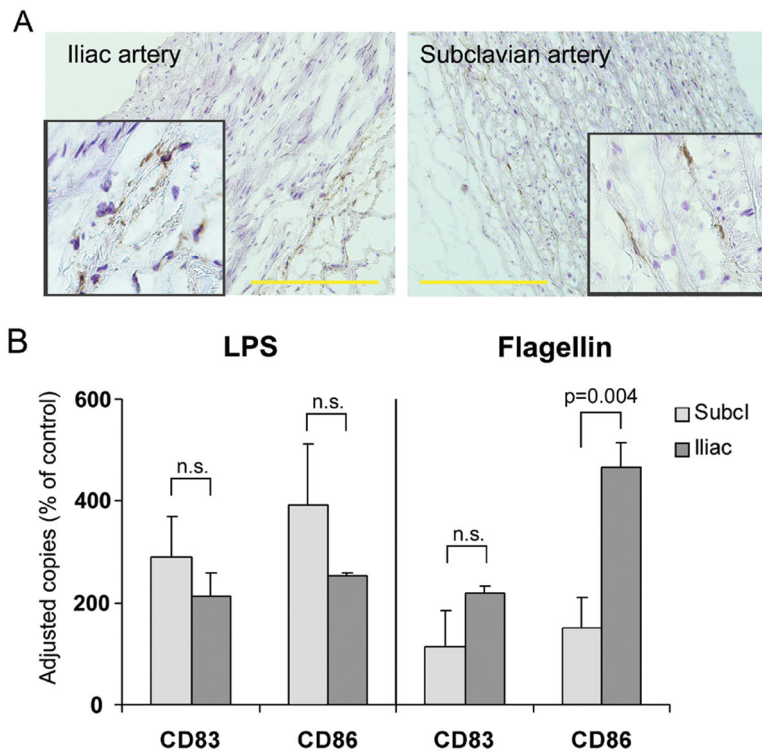


Figure 6. Vessel-specific TLR expression patterns predict responsiveness to TLR ligands
(A) Frozen sections of common iliac (left) and subclavian (right) arteries were stained with anti-TLR5 antibodies (DAB, brown). Scale bar: 100 μ m. **(B)** Responsiveness to TLR ligands was probed by stimulating with either LPS (1 μ g/mL) or flagellin (1 μ g/mL) and quantified by measuring the induction of CD83 and CD86 mRNA after 24 hours stimulation in organ culture. Results are shown as percent of control.